Supplementary Information

Correction 11-Dec-2008. E_1 = 0.0038 for ACh at –100 mV, in Supp Table 2 (misprinted as 0.038 originally)

Animated version of Figure 3a,b

A movie animation (flip-movie.wmv) can be downloaded. The first part illustrates transitions between the three states of the receptor that exist in a saturating concentration of glycine (see Fig 3a). The second part shows the same for taurine. The speed is slowed down by a factor of 10,000 (1 second per 100 μs), and is realistic apart from the fact that channels will re-open more times than is shown before reverting to the shut state. The animation shows that the smaller maximum response for taurine, compared with glycine, results mainly from the longer sojourns in the resting conformation (A_3R) with taurine, because of the slower transition rate from the resting conformation (A_3R) to the flipped (A_3F). Once the flipped conformation is reached, bursts of openings occur that are very similar for both agonists.

METHODS

Cell culture and transfection of cells.

Human embryonic kidney (HEK293) cells, obtained from the American Type Culture Collection (ATCC), were cultured and maintained in Dulbecco's modified Eagle medium containing 10% (v/v) foetal bovine serum and 1% (v/v) penicillin streptomycin solution (10,000 units/ml penicillin and 10 mg/ml streptomycin; all from Gibco, UK) at 37°C. Before experiments, cells were plated onto polylysine-coated coverslips in 35 mm culture dishes and transfected by a Ca^{2+}-phosphate co-precipitation method[1]. The DNA consisted of pcDNA3.1 plasmids (Invitrogen, The Netherlands) containing inserts encoding the human adult muscle acetylcholine receptor subunits α1, β1, δ, ε, rat glycine receptor subunits α1, β (GenBank accession numbers Y00762, X14830, X55019, X66403, AJ310834 and AJ310839, respectively), enhanced green fluorescent protein (eGFP; Clontech, UK) or no insert (non-coding plasmid). The mixture of DNA used for the cell transfection contained 5% acetylcholine receptor subunit DNA (α1, β1, δ, ε ratio 2:1:1:1), 65% eGFP DNA, and 30% non-coding plasmid or 16% glycine receptor subunit DNA (α1, β ratio either 1:4 or 1:1), 30% eGFP DNA, and 65% non-coding plasmid. Each cell culture dish was transfected with a total amount of 3 μg of DNA.

In order to avoid contamination of recordings with homomeric glycine receptors, it is necessary to transfect cells with a large excess of β subunit DNA[2], but we found that this frequently resulted in receptors that were heterogeneous at the single channel level. Receptors were more homogeneous when less β subunit DNA was used, so transfections were done with 1:1 or 1:4 ratio of α1 to β subunit DNA. This, though essential, meant that records contained variable proportions of homomeric α1 channels. Contaminant homomeric channels can be distinguished from heteromeric receptors because of their higher conductance[3,4]. However this restricted us to the higher end of the concentration range where clusters of openings from one individual channel occurred. At lower concentrations there were many isolated openings that were too short for their amplitude to be measured unambiguously.

Single channel recordings and analysis.

All recordings were performed in the cell-attached configuration using acetylcholine (ACh), tetramethylammonium (TMA) or taurine as acetylcholine receptor or glycine receptor agonists in the pipette. For recording acetylcholine receptor single-channel currents, the extracellular solution contained (mM): 5.4 NaCl, 142 KCl, 1.8 $CaCl_2$, 1.7 $MgCl_2$ and 10 HEPES (pH adjusted to 7.4 with KOH). The pipette solution was made just before recording by mixing a stock solution containing (mM) 5.4 NaCl, 142 KCl, 1.8 $CaCl_2$, 1.7 $MgCl_2$, 10 HEPES and 100 TMA or ACh (pH adjusted to 7.4 with KOH) with standard extracellular solution to obtain the required agonist concentration. For recording glycine receptor single channel currents, the extracellular solution contained (mM): 102.7 NaCl, 20 Na gluconate, 4.7 KCl, 2 $CaCl_2$, 1.2 $MgCl_2$, 10 HEPES, 14 glucose, 15 sucrose, 20 TEA-Cl (pH adjusted to 7.4 with NaOH). Just before recording, the pipette solution was prepared by mixing a stock (mM): 85 NaCl, 4.7 KCl , 2 $CaCl_2$, 1.2 $MgCl_2$, 10 HEPES, 20 TEA-Cl and 100 taurine (pH adjusted to 7.4 with NaOH) with standard extracellular solution. For the glycine receptor experiments we used HPLC-grade water (HiPerSolv, VWR, UK) in order to reduce glycine contamination. Osmolarity was 320 mOsm for all solutions.

Taurine (Fluka) was found by an HPLC assay to be contaminated by glycine (3 parts in 100,000, molar ratios). It was, therefore, purified before use (by Dr David Jane, Pharmacology Dept, University of Bristol). Taurine was passed through an ion exchange resin column, followed by crystallisation from the water eluate. This purification was found to be essential to avoid glycine-induced openings in recordings made at high taurine concentrations.

Patch pipettes were made from thick-walled borosilicate glass (GC150F, Harvard Instruments) and coated near the tip with Sylgard 184® (Dow Corning). Electrode resistance was in the range 8-15

MΩ after fire-polishing. Single-channel currents were recorded with an Axopatch 200B amplifier (Axon Instruments, California, USA), filtered at 10 kHz (sampling rate 100 kHz) and stored on the PC hard drive.

In the nicotinic receptor experiments, the high K^+ ion concentration in the extracellular solution (142 mM) means that the cell resting potential is expected to be near to 0 mV. Thus, the transmembrane potential of the patch during recording is approximately equal to the absolute value of the holding potential but of opposite sign. In the glycine receptor experiments, the cell resting potential is not artificially depolarised as the extracellular K^+ concentration is 4.7 mM, hence the real patch transmembrane potential during recording will be more negative than –100 mV (i.e. –100 mV plus the resting membrane potential of the HEK293 cell, typically between –20 and –40 mV[5]). The observed amplitude of the currents for heteromeric receptors for taurine was 2.9 ± 0.1 pA (n = 14), much the same as for glycine (3.1 pA[6]).

We did not correct for junction potential, as with our solutions this is expected to be at most 1 mV (as calculated in Clampex 9, Axon Instruments). All experiments were done at 19 - 21°C.

For off-line analysis, data were filtered at 3 – 8 kHz and sampled at 33 – 100 kHz. Open times, shut times, and amplitudes were idealized with SCAN (http://www.ucl.ac.uk/pharmacology/dc.html) and dwell-time distributions were fitted with mixtures of exponential densities using the EKDIST program after imposing a resolution of 20-100 μs. For each recording, 10,000–20,000 transitions were fitted.

Because we do not know the number of channels in the patch, it is essential for model fitting to divide the idealised single channel record in to stretches that originate, almost certainly, from one individual channel. When opening are sparse (at low agonist concentrations) such stretches are short, each consisting of a single activation (short burst of openings) of the channel, but when P_{open} is high, long stretches of data with no second channel opening can be obtained. The division of the record into one-channel stretches was achieved by defining a critical shut time, t_{crit}, on the basis of inspection of the shut time distribution. Sometimes this process can be ambiguous but our conclusions do not depend critically on this choice. The shut time distributions are shown only up to t_{crit}, because shut times longer than this were not used for fitting.

Selection of data records

Recordings made at different concentrations of agonist were grouped arbitrarily into sets for simultaneous fitting. Each set included one recording at each of the concentrations used (four for ACh at -100 mV, three for all other agonists) and the sets were independent, i.e. each individual patch was included in only one set. The data reported here are the result of fitting three such replicate sets (two for ACh and TMA at +80 mV). Records that showed obvious heterogeneity, as judged mainly by occurrence of clusters of openings with abnormally high P_{open}, were excluded. Two recordings (one for ACh and one for TMA) were excluded on the grounds that they gave values for association rate constants greater than 10^9 $M^{-1}s^{-1}$, a value that is physically impossible.
The temporal resolution of TMA-activated single-channel records at negative transmembrane potential rapidly worsened at concentrations higher than 1 mM as the reduction in the apparent channel amplitude (Fig. 4a) meant that a progressively larger fraction of short closings was missed.

The main conclusion, that partial agonists showed a low flipping constant (F) rather than a low gating constant (E), was insensitive to the choice of which sets to exclude. The less well-defined constants that refer to receptors that are not fully-liganded were rather more sensitive, but their exact values are not crucial for our argument.

Allowance for channel blocking action in fits of acetylcholine and TMA data at negative membrane potentials

Both nicotinic agonists produced channel block at negative potentials. The fact that we get very similar results at positive membrane potentials where block is essentially absent rules out channel block as an explanation for our results, but it is necessary to consider its effect at negative potentials.

The case of ACh is the simplest. With ACh as agonist, the channel blockages are sufficiently long that some of them can be detected. The blocked state (A_2R^*B in Supplementary Fig. 2) can therefore be included as a discrete state and the association and dissociation rate constants for the open channel block fitted as free parameters. The results are shown in Supplementary Table 2. The association rate constant, k_{+B}, was 8.6×10^7 $M^{-1}s^{-1}$ and the dissociation rate constant implied a mean blockage length of 10 μs.

TMA is somewhat more difficult, because essentially all the channel blockages that it produces seem to be too short to be resolved. Figure 4d shows that at the highest TMA concentration fitted (10 mM), channels are blocked for about half the time at –80 mV, because the apparent channel

amplitude is approximately halved. If we assume the simplest mechanism (pure open channel block) and we make the reasonable supposition that the association rate constant for TMA block is similar to that measured for ACh (8.6×10^7 M^{-1} s^{-1}), the following predictions can be made, for 10 mM TMA. An apparent opening would consist of a burst of roughly 280 very brief openings and blockages, each with mean duration about 1.5 μs. Filtering would make this look like a single opening with half the true amplitude. All the blockages would be too short to be resolved (less than a 1 in 10^6 chance of any blockage being resolved in an apparent opening, with a resolution of 30 μs).

We therefore attempted fits that assumed very fast selective open-channel block. When the transition rates between two (or more) states are very fast then the states can be pooled into a single compound state for the purposes of kinetics. In this case the open and blocked states, A_2R^* and A_2R^*B, are pooled. This has the effect of making the shutting rate α_2 appear to be concentration-dependent. Therefore α_2 is replaced for all calculations by $\alpha_2/(1 + [B]/K_B)$, because the fraction of the time for which the compound state is not blocked, and therefore available to shut, is $1/(1 + [B]/K_B)$ where [B] is the blocker (agonist) concentration. The rates of block and unblock do not appear in this, but only the equilibrium constant for block, because of the assumption that these rates are so fast that the blocking reaction is at equilibrium throughout. We found that fits with the fast block correction (not shown) were somewhat less good than those without it. This suggests that TMA is not a pure open channel blocker[7]. If it were, we would also expect that at a concentration of K_B (about 10 mM) the length of the apparent opening would be doubled[8]. We failed to observe this lengthening, presumably because the TMA-blocked channel can shut[9,10]. The fits in Figure 5 and Supplementary Figure 4 were done without the fast block correction. It is important to note that both fits gave the same qualitative result, namely that partial agonism depends mainly on poor flipping rather than inefficient opening.

Extended discussion of results

Agonist affinity for the open states

Dissociation of agonist from open states must, in principle, be possible so it may be asked why the open states are not connected in the flip mechanism (Figs. 2a and 5a). The main reason is that dissociation appears to be too slow to be detected[6], and it is not sensible to include in the fitting process parameters that cannot be estimated reliably from the data. If the open states are joined, then new cycles are created, and if these cycles are assumed to obey microscopic reversibility, then this places an extra constraint on the mechanism. In the case of the glycine receptor, this constraint

would mean, for example, that the ratio of the open-shut equilibrium constant for triply- and doubly-occupied receptors (E_3/E_2) should be the same as the ratio for doubly- and singly-occupied receptors (E_2/E_1). These ratios were not found to be the same[6], so the extra constraint produced by joining the open states actually reduced somewhat the quality of the fit. This could be a result of the flip mechanism being still not sufficiently detailed. It might also result from there being some interaction between ion flow and the open-shut conformation change that results in a breach of microscopic reversibility. This is an interesting question for future investigation, but it does not affect the conclusions of this paper.

Fits for the heteromeric glycine receptor

Supplementary Table 1 shows the complete results of the global fits to sets of observations with glycine and taurine. It was not possible to use taurine concentrations lower than 1 mM because openings were sparse and occurred in short bursts. Many bursts were so short that heteromeric and homomeric openings could not be distinguished unambiguously. So it is not surprising that initial fits suggested that there were few monoliganded openings in our records. Therefore monoliganded flipped and open states were not included in the mechanism in the final fits (Fig. 2a, grey regions).

With glycine as agonist, all 12 free rate constants are quite well determined. With taurine as agonist, the rates for the triliganded receptor are also quite precise, but those for the diliganded receptor are less precise. That is because it was necessary to limit our fits to high concentrations of taurine (1 mM and higher), and calculations with the fitted rate constants suggest that most receptors will be triliganded even at 1 mM. This is confirmed in Supplementary Figure 1, which completes the display of the global fitting of the taurine data shown in Figure 2 of the paper. The conditional mean open time shows little dependence on adjacent shut time, as expected if most receptors are fully liganded, and this outcome is predicted by the calculated conditional means calculated from the fitted rate constants (open symbols and dashed lines).

The value of γ_2 is faster than we can expect to estimate; this value is determined by microscopic reversibility and all that can be said is that the lifetime of the diliganded flipped conformation appears to be very small. This outcome is not at all critical for our conclusions, which depend on the properties of the fully-liganded receptor.

The values in Supplementary Table 1 give the basis for the conclusion (main paper) that the affinities of glycine and taurine for the resting state (K) are comparable, but that the affinity of taurine for the flipped state (K_F) is much lower than that of glycine. This accounts (via microscopic reversibility) for the finding that the flipping equilibrium constant, F_3, is very much smaller for taurine than for glycine. The flipping equilibrium constant is smaller for taurine than glycine by a factor of about 180, both because the rate of entry into the flipped state (δ_3) is slower (by a factor of 28) and because the rate of return to the resting conformation (γ_3) is faster (by a factor of about 6). The reason for the higher affinity of glycine for the flipped conformation is that the association rate constant for glycine (k_{F+}), 1.50×10^8 $M^{-1}s^{-1}$, is almost 63 times faster than that for taurine.

Fits for the nicotinic receptor

The complete numerical results for fits with acetylcholine and with TMA at both −80 mV and at +80 mV are shown in Supplementary Table 2. The tests for the quality of the fits are shown in Supplementary Figures 2 - 5. These Figures show the apparent open and shut times distributions that are predicted by the fit, superimposed on histograms of the observations, for each of the concentrations in one of the sets of data that contributes to the averages in the Tables (the P_{open} curves that are predicted by the fit are shown in the main paper, and are seen to describe the observations well). The Supplementary Figures show also the predicted and observed conditional mean open time plots, as described in the legend of Supplementary Figure 1. The flatness of most of these plots suggests, as for the glycine receptor experiments, that most receptors are fully liganded under the conditions we use. It is, therefore, not surprising that the rate constants for monoliganded receptors are less precise than those for diliganded receptors. This is of secondary importance because it is the latter than we need to test our hypothesis.

The fits for ACh at −100 mV (Supplementary Fig. 2) are excellent at all concentrations. Records with ACh have not previously been fitted with the flip model. The values of the open-shut equilibrium constant, E_2, are very similar for ACh and for TMA at both negative and positive membrane potentials, as are the underlying rate constants. But the flipping equilibrium constant, F_2, for the partial agonist, TMA, is smaller than that for ACh by a factor of 27 (at negative potentials) or 18 (at positive potential), again largely as a result of the transition from resting to flipped being slower for TMA than for ACh. The gating constant, E_2, is reduced at +80 mV by about the amount (69 mV for e-fold change) expected from the voltage dependence of the opening and shutting rates, but the flipping equilibrium constant is reduced too, and remains much (47-fold) smaller than the open-shut equilibrium constant. This provides confirmation of our thesis that partial agonism is a

property of the flipping step rather that the open-shut conformation change step, under conditions where the result is unaffected by the powerful channel block produced by agonist at negative membrane potentials.

Results with ACh can usually be fitted quite well with the assumption that the binding sites are independent. The two sites are certainly physically different, though reports about the extent to which this is detectable with ACh itself are quite inconsistent. In any case, ACh does not show the strong apparent interaction between binding sites that provided the initial incentive to develop the flip mechanism for glycine receptors[6]. This is borne out by the finding that ACh (unlike glycine) has only a slightly higher affinity for the flipped conformation than for the resting state (Supplementary Table 2).

The fits for the acetylcholine records at positive membrane potential (Supplementary Fig. 3) are reasonably good at all concentrations. However, it should be mentioned that the single-channel activations by ACh at +80 mV were difficult to idealise unambiguously, especially at the higher ACh concentration. In these records, activations occurred as barrages of short openings and shuttings (see the bottom trace in Supplementary Fig. 3a), which were mostly too short at our bandwidth to reach the full open or full shut level. Because of this, we imposed on the acetylcholine records at +80 mV a much more conservative resolution of 100 μs. We were concerned that including these records would lead to inaccuracy in the estimation of rate constants. However, we found that the coefficients of variation of the rate constant estimates were still reasonably low (see Supplementary Table 2). In addition to that, we also measured the P_{open} by integration of the raw data trace, a method that needs only an estimate of channel amplitude, but which is independent of idealisation and of filtering. These P_{open} values were similar to those measured by idealisation. Furthermore, the reduction of the maximum P_{open} at positive potentials is similar to that reported previously[11] (for frog muscle). The predictions of the fits of the flip model described satisfactorily the experimental observations, including the P_{open} curve, in which open probabilities were estimated independently of the idealisation method. This encourages us to trust the results, though they cannot be quite as reliable as those at negative potentials. The results were very similar to those at negative potentials.

One interesting aspect of the results in Supplementary Table 2 is that the main channel opening rate, β_2, seems to be almost as voltage-dependent as the shutting rate, α_2 for both ACh and TMA. Previous reports[12,13] have suggested that the opening rate is almost independent of membrane potential, whereas the shutting rate, α_2, increases strongly with depolarisation, changing *e*-fold for

each 55 – 80 mV. The voltage dependence of the overall resting-open transition also has a contribution from the flipping rate constants which change with voltage in the same direction, but to a lesser extent than the open-shut rates constants. Insofar as our mechanism describes reality better than those used before, it may be that these are better estimates of the true rate constants.

Implications of the results for the rise time of macroscopic responses

The existence of an intermediate shut state of the fully-occupied receptor, the flip state, must inevitably slow the rise time of the response to a step to a large agonist concentration, including the rise time of synaptic currents. It is important to be sure that the predictions of the flip model are consistent with what is known about response rise times.

In the case of the glycine receptor, it was shown by Burzomato *et al*. (2004)[6] that the rate constants inferred from single channel analysis predicted accurately the shape of miniature synaptic currents mediated by glycine in rat spinal motor neurones. In contrast, responses to fast concentration jumps on outside-out patches were rather faster than predicted from recordings in the cell-attached mode and this appears to be an artefact of patch excision (Pitt *et al*., submitted).

There have been many more estimates of rise time for the muscle type nicotinic receptor than for the glycine receptor. Most estimates of the fully-liganded opening rate constant, β_2, are in the range 40,000 to 80,000 s^{-1} [14-17]. Our estimate of β_2 in the context of the flip mechanism is very similar to that estimated from the fastest concentration jumps by Maconochie and Steinbach (1998)[15]. Because of the presence of the flip state, our prediction for the rise time of the response to high concentrations is slower.

Simulated concentration jump responses using our estimates of flipping and open-shut rate constants give rise time constant values between 40 and 70 μs for ACh. This prediction is close to the mean first passage time from the fully-liganded resting state (A_2R) to the open state, as expected when high concentration makes binding very fast. This mean first passage time can be calculated from equation 3.91 of Colquhoun & Hawkes (1982)[18] by substitution of the appropriate initial vector in place of the equilibrium vector, ϕ_s. This rise time prediction is still quite fast enough to be consistent with even the fastest estimates of the rise times of miniature synaptic currents[19], and with most concentration jump experiments too. It is slower than would be expected from the fastest jump experiments[15]. This could be a consequence of artefactual speeding of the response when outside-out patches are excised (as seen with the glycine receptor), or simply a consequence of the fact that we are using the human receptor rather than the mouse receptor.

Φ value analysis

The technique of rate-equilibrium free energy relationship analysis[20] can be applied to single channel data in order to obtain information on the relative timing of movements for the different parts of the channel[21-23]. In the first application of this technique to channels, Grosman *et al*. (2000)[21] investigated the resting-open reaction of the fully-liganded muscle nicotinic channel by activating it by a series of agonists. They found a high Φ value (0.93). This result was interpreted as meaning that the area perturbed by the experimental manipulation (i.e. the ligand binding site) moved very early in the chain of movements that convert binding to opening[22,23].

The mechanisms that we fitted are more detailed than that used in the original Φ value analysis, as they include three distinguishable states for the saturated receptor (resting, flipped and open; Fig. 3) rather than two (resting and open). It is possible that our flipped state represents a particularly stable reaction intermediate among the microstates that are thought to populate the flattish, rugged energy landscape at the transition state[24]. Presumably the flip state would correspond to the first of the five blocks of amino acids that Auerbach's group[25] identifies, or the first state in rapid equilibrium with one or more of the following intermediates.

In order to calculate the Φ value for the agonist perturbation in the glycine channel in a manner comparable to that of Grosman *et al*. (2000)[21], we have to obtain both the effective forward rate and the effective equilibrium constant for the whole transition between resting and open (denoted β_{eff} and E_{eff}), from the results of our fits for the two agonists. When our system is reduced to two states, shut and open, the effective equilibrium constant is $E_{\text{eff}} = EF/(1 + F)$ where E and F refer to the fully-liganded receptor. This must be equal to $\beta_{\text{eff}}/\alpha$ so the effective opening rate constant is

$$\beta_{\text{eff}} = \beta\left(\frac{F}{1+F}\right)$$

This is easily shown to be the high-concentration limit of the reciprocal of the mean of all shut times, as calculated from Equation 3.91 of Colquhoun & Hawkes, 1982[18].

With these results we can calculate Φ values as the slope of the graph of $\log(\beta_{\text{eff}})$ against $\log(E_{\text{eff}})$, by least squares fit of a straight line to the two groups of points from replicate experiments with taurine and glycine. We obtained a Φ value of 0.71 ± 0.06 (n = 3 replicate experiments for both glycine and taurine), somewhat smaller than the value of 0.93 reported by Grosman *et al*. (2000)[21] with a large series of agonists on the nicotinic channel. This is because the change in E_{eff} was in

part due to a change in the shutting rate constant for the fully liganded receptor, α. We found a modest, but consistent, difference in α_3 between glycine and taurine by a factor of about 2 on average (Supplementary Table 1) and this is sufficient to reduce Φ below 1.

When the same procedure was repeated for the nicotinic receptor with acetylcholine and TMA, we obtained Φ values very close to unity, entirely consistent with those reported by Grosman *et al*. (2000)[21]. We found $\Phi = 1.02 \pm 0.06$ at negative membrane potentials ($n = 3$ replicate experiments for both agonists) and 1.02 ± 0.08 at positive potentials ($n = 2$ replicates). This suggests that, in the case of the nicotinic receptor, the flip state is likely to be a direct physical manifestation of sojourns the first block of amino acids to move during activation as postulated by Chakrapani *et al*. (2004)[26].

Supplementary information- References

1. Groot-Kormelink, P. J., Beato, M., Finotti, C., Harvey, R. J. & Sivilotti, L. G. Achieving optimal expression for single channel recording: a plasmid ratio approach to the expression of α1 glycine receptors in HEK293 cells. *J. Neurosci. Meth.* **113**, 207-214 (2002).

2. Burzomato, V., Groot-Kormelink, P. J., Sivilotti, L. G. & Beato, M. Stoichiometry of recombinant heteromeric glycine receptors revealed by a pore-lining region point mutation. *Recept. Chann.* **9**, 353-361 (2003).

3. Bormann, J., Rundström, N., Betz, H. & Langosch, D. Residues within transmembrane segment M2 determine chloride conductance of glycine receptor homo- and hetero-oligomers. *EMBO J.* **12**, 3729-3737 (1993).

4. Beato, M., Groot-Kormelink, P. J., Colquhoun, D. & Sivilotti, L. G. Openings of the rat recombinant α1 homomeric glycine receptor as a function of the number of agonist molecules bound. *J. Gen. Physiol.* **119**, 443-466 (2002).

5. Thomas, P. & Smart, T. G. HEK293 cell line: a vehicle for the expression of recombinant proteins. *J. Pharmacol. Toxicol. Methods* **51**, 187-200 (2005).

6. Burzomato, V., Beato, M., Groot-Kormelink, P. J., Colquhoun, D. & Sivilotti, L. G. Single-channel behavior of heteromeric α1β glycine receptors: an attempt to detect a conformational change before the channel opens. *J. Neurosci.* **24**, 10924-10940 (2004).

7. Akk, G. & Steinbach, J. H. Activation and block of mouse muscle-type nicotinic receptors by tetraethylammonium. *J. Physiol* **551**, 155-168 (2003).

8. Neher, E. & Steinbach, J. H. Local anaesthetics transiently block currents through single acetylcholine-receptor channels. *J. Physiol. (Lond.)* **277**, 153-176 (1978).

9. Lingle, C. Blockade of cholinergic channels by chlorisondamine on a crustacean muscle. *J. Physiol. (Lond.)* **339**, 395-417 (1983).

10. Gurney, A. M. & Rang, H. P. The channel-blocking action of methonium compounds on rat submandibular ganglion cells . *Br. J. Pharmacol.* **120**, 471-490 (1984).

11. Colquhoun, D. & Ogden, D. C. Activation of ion channels in the frog end-plate by high concentrations of acetylcholine. *J. Physiol. (Lond.)* **395**, 131-159 (1988).

12. Colquhoun, D. & Sakmann, B. Fast events in single-channel currents activated by acetylcholine and its analogues at the frog muscle end-plate. *J. Physiol. (Lond.)* **369**, 501-557 (1985).

13. Auerbach, A., Sigurdson, W., Chen, J. & Akk, G. Voltage dependence of mouse acetylcholine receptor gating: different charge movements in di-, mono- and unliganded receptors. *J. Physiol. (Lond.)* **494 (Pt 1)**, 155-170 (1996).

14. Sine, S. M. & Steinbach, J. H. Activation of acetylcholine receptors on clonal mammalian BC3H-1 cells by high concentrations of agonist. *J. Physiol. (Lond.)* **385**, 325-359 (1987).

15. Maconochie, D. J. & Steinbach, J. H. The channel opening rate of adult- and fetal-type mouse muscle nicotinic receptors activated by acetylcholine. *J. Physiol. (Lond.)* **506**, 53-72 (1998).

16. Hatton, C. J., Shelley, C., Brydson, M., Beeson, D. & Colquhoun, D. Properties of the human muscle nicotinic receptor, and of the slow-channel myasthenic syndrome mutant epsilonL221F, inferred from maximum likelihood fits. *J. Physiol. (Lond.)* **547**, 729-760 (2003).

17. Salamone, F. N., Zhou, M. & Auerbach, A. A re-examination of adult mouse nicotinic acetylcholine receptor channel activation kinetics. *J. Physiol. (Lond.)* **516**, 315-330 (1999).

18. Colquhoun, D. & Hawkes, A. G. On the stochastic properties of bursts of single ion channel openings and of clusters of bursts. *Phil. Trans. R. Soc. Lond. B* **300**, 1-59 (1982).

19. Stiles, J. R., Van, H. D., Bartol, T. M., Jr., Salpeter, E. E. & Salpeter, M. M. Miniature endplate current rise times less than 100 μs from improved dual recordings can be modeled with passive acetylcholine diffusion from a synaptic vesicle. *Proc. Natl. Acad. Sci. U. S. A* **93**, 5747-5752 (1996).

20. Fersht, A. R. Relationship of Leffler (Bronsted) α values and protein folding Φ values to position of transition-state structures on reaction coordinates. *Proc. Natl. Acad. Sci. U. S. A.* **101**, 14338-14342 (2004).

21. Grosman, C., Zhou, M. & Auerbach, A. Mapping the conformational wave of acetylcholine receptor channel gating. *Nature* **403**, 773-776 (2000).

22. Zhou, Y., Pearson, J. E. & Auerbach, A. Φ-value analysis of a linear, sequential reaction mechanism: theory and application to ion channel gating. *Biophys. J.* **89**, 3680-3685 (2005).

23. Auerbach, A. How to turn the reaction coordinate into time. *J. Gen. Physiol* **130**, 543-546 (2007).

24. Auerbach, A. Gating of acetylcholine receptor channels: brownian motion across a broad transition state. *Proc. Natl. Acad. Sci. U. S. A.* **102**, 1408-1412 (2005).

25. Purohit, P., Mitra, A. & Auerbach, A. A stepwise mechanism for acetylcholine receptor channel gating. *Nature* **446**, 930-933 (2007).

26. Chakrapani, S., Bailey, T. D. & Auerbach, A. Gating dynamics of the acetylcholine receptor extracellular domain. *J. Gen. Physiol.* **123**, 341-356 (2004).

27. Colquhoun, D., Dowsland, K. A., Beato, M. & Plested, A. J. How to impose microscopic reversibility in complex reaction mechanisms. *Biophys. J.* **86**, 3510-3518 (2004).

Supplementary Tables 1 and 2

The values shown are the estimates of the rate constants from the fits of mechanisms shown in Figure 2 and Supplementary Figure 1 (taurine), Figure 5 and Supplementary Figures 4 and 5 (TMA –80 mV and +80 mV) and Supplementary Figures 2 and 3 (ACh –100 mV and +80 mV, respectively). The names of the rate constants are as shown in the state diagrams in the Figures. Values for glycine, shown for reference, are from Burzomato *et al.*, 2004[12].

Values shown are the averages of the rate constant estimates obtained from fits to several independent data sets, three each for taurine, ACh and TMA at negative potential and two each for ACh and TMA at positive potentials, together with the error in the estimates, expressed as coefficient of variation (right hand columns). Each set contained patches at three different agonist concentrations (four for glycine and ACh): 1 to 100 mM for taurine; 10, 30, 100, and 1,000 μM for glycine; 0.05 to 64 μM for ACh at -100 mV; 3 to 300 μM for ACh at +80 mV; 0.1 to 30 mM for TMA at -80 mV; 0.3 to 100 mM for TMA at +80 mV. Equilibrium constants were calculated separately as the ratios of the appropriate rate constants in each of the replicate sets and the individual equilibrium constants were then averaged.

All rate constants were fitted freely, except for the constraint for microscopic reversibility imposed by the presence of cycles in the mechanisms (see Colquhoun *et al*., 2004[27]).

Supplementary Table 1. Fitted rate constants for the glycine receptor.

Rate constant	Units	Glycine		Taurine	
α_2	s^{-1}	2,100	±12%	1,150	±61%
β_2	s^{-1}	28,000	±17%	250	±92%
α_3	s^{-1}	7,000	±18%	14,500	±7%
β_3	s^{-1}	129,000	±4%	133,000	±3%
γ_2	s^{-1}	18,000	±14%	739,000	±35%
δ_2	s^{-1}	6,800	±6%	96,000	±71%
γ_3	s^{-1}	900	±26%	5,170	±11%
δ_3	s^{-1}	20,900	±3%	740	±10%
k_{F+}	$M^{-1}\ s^{-1}$	1.50×10^8	±5%	2.38×10^6	±47%
k_{F-}	s^{-1}	1,200	±12%	1,230	±21%
$k_{-1} = k_{-2} = k_{-3}$	s^{-1}	300	±6%	220	±19%
$k_{+1} = k_{+2} = k_{+3}$	$M^{-1}\ s^{-1}$	5.9×10^5	±6%	2.2×10^5	±20%
E_2 $(= \beta_2/\alpha_2)$	-	13	± 9%	0.14	± 56%
E_3 $(= \beta_3/\alpha_3)$		20	± 16%	9.2	± 3%
F_2 $(= \delta_2/\gamma_2)$	-	0.4	± 15%	0.12	± 51%
F_3 $(= \delta_3/\gamma_3)$	-	27	± 31%	0.15	± 20%
K $(= k_{-1}/k_{+1})$	μM	520	± 12%	1,040	± 16%
K_F $(= k_{F-}/k_{F+})$	μM	8	± 14%	690	± 27%

Supplementary Table 2. Fitted rate constants for the nicotinic acetylcholine receptor.

Rate constant	Units	ACh; -100 mV		ACh; +80 mV		TMA; -80 mV		TMA; +80 mV	
α_1	s^{-1}	17,700	±24%	12,200	±21%	330	±97%	830	±93%
β_1	s^{-1}	40	±88%	54,000	±24%	2	±42%	2	±49%
α_2	s^{-1}	2,560	±5%	9,550	±11%	2,520	±12%	9,100	±15%
β_2	s^{-1}	87,700	±3%	29,400	±4%	70,500	±9%	25,000	±3%
γ_1	s^{-1}	128,000	±98%	929,000	±5%	146,000	±71%	180,000	±89%
δ_1	s^{-1}	295,000	±96%	2,990	±21%	540	±98%	5,700	±87%
γ_2	s^{-1}	8,400	±54%	16,100	±19%	12,600	±25%	19,900	±8%
δ_2	s^{-1}	22,900	±22%	16,900	±21%	1,470	±27%	1,200	±19%
k_{F+}	$M^{-1}\ s^{-1}$	2.03×10^8	±26%	8.43×10^8	±18%	2.90×10^8	±68%	4.1×10^6	±11%
k_{F-}	s^{-1}	3,240	±39%	108	±2%	15,500	±32%	4,900	±7%
$k_{-1} = k_{-2}$	s^{-1}	9,480	±48%	27,900	±21%	9,730	±30%	1,800	±48%
$k_{+1} = k_{+2}$	$M^{-1}\ s^{-1}$	2.71×10^8	±59%	6.51×10^8	±25%	5.65×10^6	±56%	7.4×10^5	±30%
k_{+B}	$M^{-1}\ s^{-1}$	8.6×10^7	±14%	-	-	-	-	-	-
k_{-B}	s^{-1}	95,300	±3%	-	-	-	-	-	-
E_1 $(= \beta_1/\ \alpha_1)$	-	0.0038	± 94%	4.4	±3%	0.046	± 81%	0.020	± 98%
E_2 $(= \beta_2/\alpha_2)$		34.4	± 5%	3.1	±15%	28.1	± 2%	2.8	± 12%
F_1 $(= \delta_1/\gamma_1)$	-	2.3	± 55%	0.003	±27%	0.014	± 79%	0.03	± 7%
F_2 $(=\delta_2/\gamma_2)$	-	3.8	± 27%	1.1	±2%	0.14	± 40%	0.06	± 11%
K $(= k_{-1}/\ k_{+1})$	μM	40.1	± 13%	43	±5%	3,000	± 40%	2,310	± 21%
K_F $(= k_{F-}/\ k_{F+})$	μM	20.7	± 46%	0.13	±21%	340	± 83%	1,240	± 18%
K_B $(= k_{-B}/\ k_{+B})$	mM	1.2	± 18%	-	-	-	-	-	-

Supplementary Figure 1.

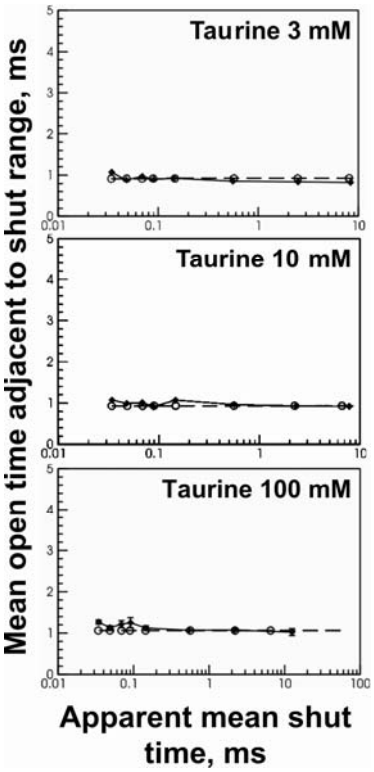

The lack of correlation between adjacent open and shut times is well predicted by the fit of the taurine data.

The plots show as filled symbols the mean apparent duration of openings that were adjacent to shut times in a specified range. The open symbols and the dashed lines are the predictions of the fitted model. The prediction agrees reasonably well with the experimental points. These plots illustrate the correlation between the adjacent open and shut times. Apparently, there is little such correlation in records of taurine-bound glycine receptor activations in the range of concentrations between 3 to 100 mM, as mean apparent open times are approximately 1 ms, irrespective of whether they are near a short shutting (points on the left) or a long one. This is because of the paucity of openings from receptors that are less than triply-liganded.

Supplementary Figure 2.

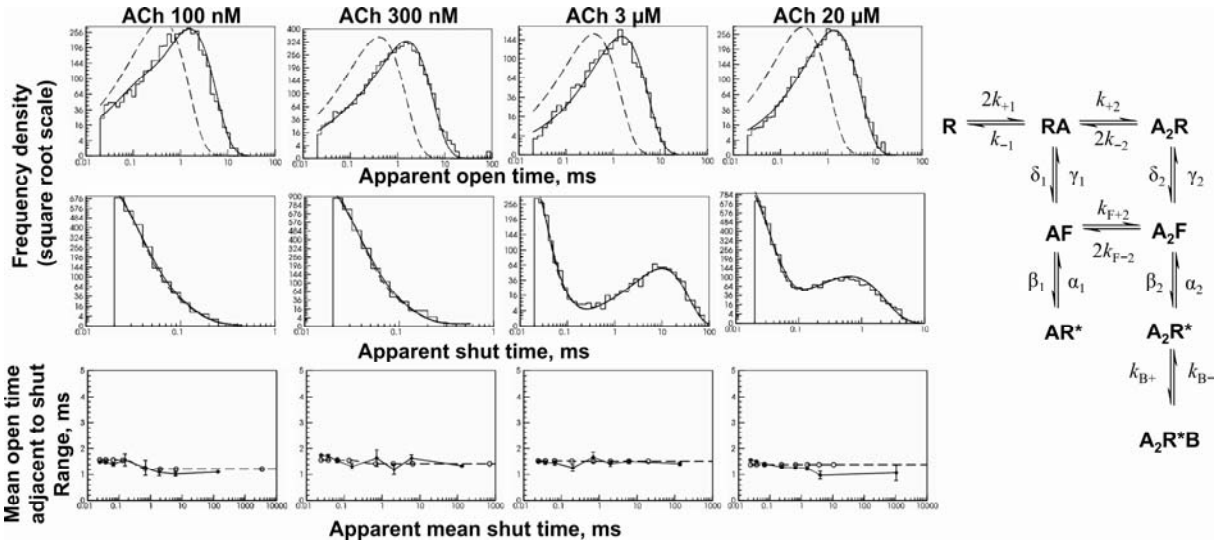

The 'flip' mechanism describes well channel activations evoked by a range of ACh concentrations at −100 mV. The mechanism is shown on the right and explicitly includes a blocked state, linked to the diliganded open state.

The plots show the experimental apparent open (top row) and shut (middle row) time distributions (stepwise lines) at four ACh concentrations (0.1, 0.3, 3 and 20 μM). The frequency densities for the distributions of apparent dwell times calculated from the fitted rate constants at our experimental resolution are the solid lines superimposed to the data histograms. The dashed lines are the distributions predicted if resolution were perfect and no events were missed. The difference between the two shows how essential it is to have full missed event correction in the fitting process, particularly for open times. The bottom row of graphs show the mean apparent duration of openings that were adjacent to shut times in a specified range (filled symbols). The predictions of the fitted model are shown as open symbols and dashed lines.

Supplementary Figure 3.

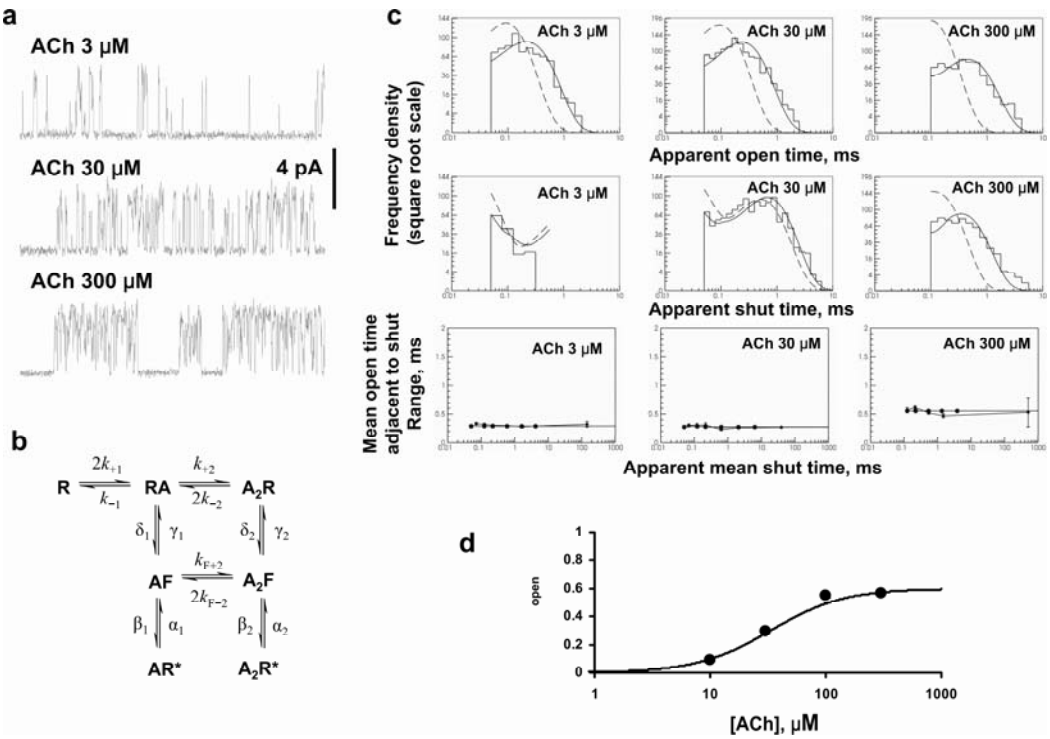

The results of the maximum likelihood fit of the 'flip' mechanism to the openings of the nicotinic receptor activated by ACh recorded at +80 mV.

a, Single-channel currents (opening upwards) produced by increasing concentrations of ACh at +80 mV transmembrane potential. At high concentrations, activations become more closely spaced, and open probability increases. b, Mechanism fitted to nicotinic receptor activations by ACh at +80 mV. c, The plots show the experimental apparent open (top row) and shut (middle row) time distributions (stepwise lines) at three ACh concentrations (3, 30 and 300 μM), together with the predictions of the fit (details as in Supplementary Figure 2). d, The results of the fit predict accurately the channel open probability.

Supplementary Figure 4.

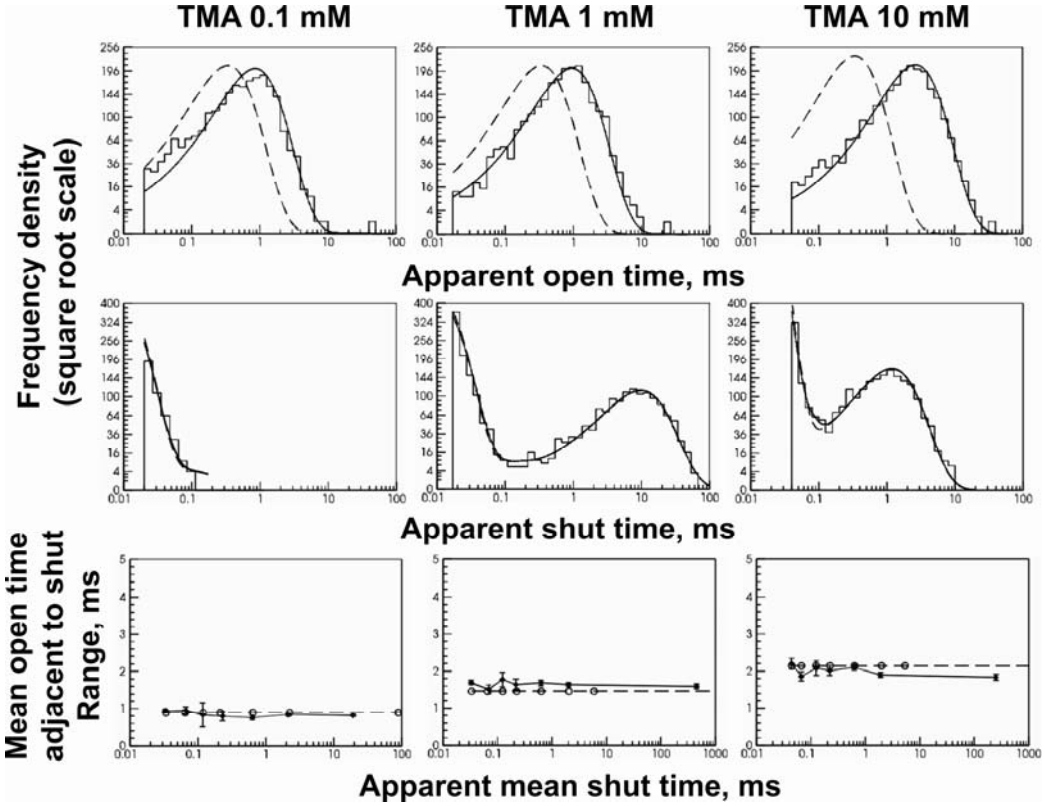

The complete results of the maximum likelihood fit of the 'flip' mechanism to the idealised records of openings of the nicotinic receptor activated by TMA at −80 mV. Same set and mechanism as in Figure 5c: all distributions and plots are shown here, better to allow a judgement of the quality of the global fit. The top and middle rows are distributions of apparent open and shut times (see legend to Supplementary Figure 2) and the bottom row are correlation plots (see legend to Supplementary Figure 1).

Supplementary Figure 5.

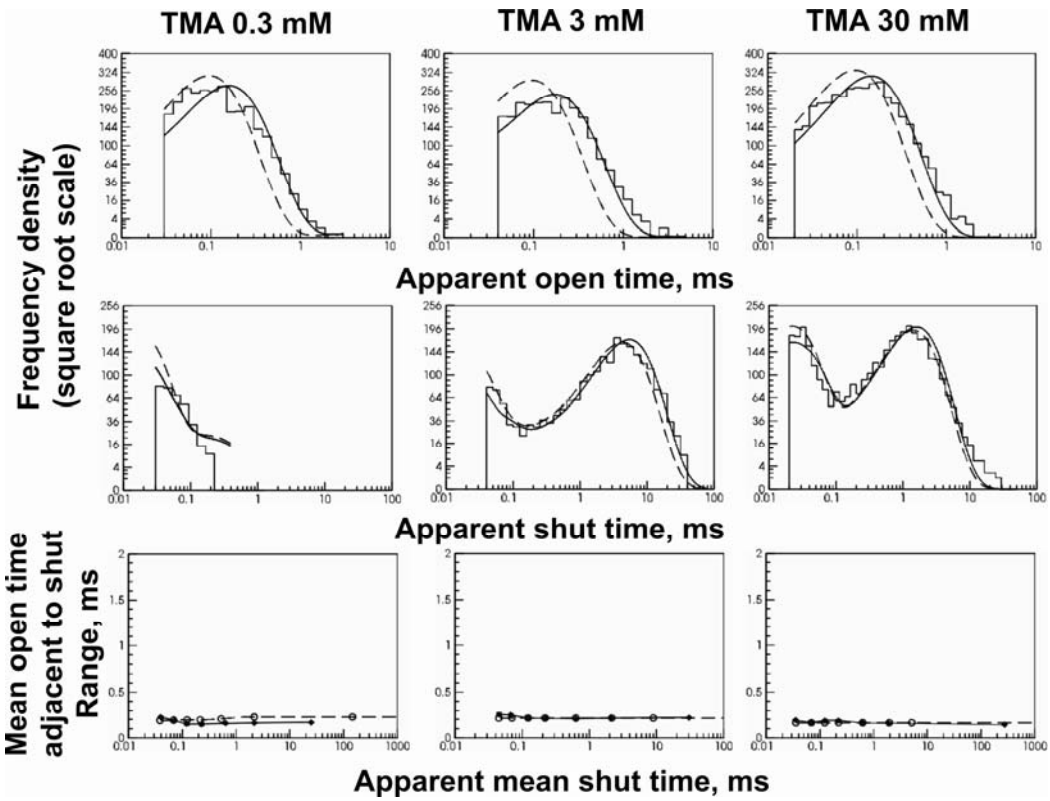

The complete results of the maximum likelihood fit of the 'flip' mechanism to the openings of the nicotinic receptor activated by TMA recorded at +80 mV. Same sets and mechanism as in Figure 5d: all distributions and plots are shown here, better to allow a judgement of the quality of the global fit. The top and middle rows are distributions of apparent open and shut times (see legend to Supplementary Figure 2) and the bottom row are conditional mean apparent open time plots (see legend to Supplementary Figure 1).